# Examining the effect of a binding-energy-dependent clusterization algorithm on isospin-sensitive observables in heavy-ion collisions

Sanjeev Kumar and Y. G. Ma

Phys. Rev. C **91**, 034612 — Published 23 March 2015

DOI: 10.1103/PhysRevC.91.034612

# Examining the effect of binding energy dependent clusterization algorithm on isospin sensitive observables in heavy-ion collisions

Sanjeev Kumar *[1] and Y. G. Ma[2,†]

[1]*Physics and Ballistics Division, State Forensic Science Laboratory, Himachal Pradesh, Shimla Hills, Junga 171218, India*

[2]*Shanghai Institute of Applied Physics, Chinese Academy of Sciences, Jiading Campus, Shanghai 201800, China*

(Dated: March 5, 2015)

The phase space obtained using Isospin Quantum Molecular Dynamical (IQMD) Model is analyzed by applying the binding energy cut in the most commonly and widely used secondary cluster recognization algorithm. In addition, for the present study, the energy contribution from momentum dependent and symmetry potentials is also included during the calculation of total binding energy, which was absent in clusterization algorithms used earlier.The stability of fragments and isospin effects are explored by using the new clusterization algorithm. The findings are summarized as follow: (1) It identifies the fragments at quite early time. (2) It is more sensitive for free nucleons and light charged particles compared to intermediate mass fragments, which results in the enhanced (reduced) production of free nucleons (LCPs). (3) It has affected the yield of isospin sensitive observables neutrons (n), protons (p), $^3H$, $^3He$ and single ratio [$R(n/p)$] to a greater extent in mid-rapidity and low kinetic energy region. In conclusion, the induction of binding energy cut in the clusterization algorithm is found to play a crucial role in the study of isospin physics. This study will give another direction for the determination of symmetry energy in heavy-ion collisions at intermediate energies.

PACS numbers: 25.70.Mn, 21.65.Ef, 24.10.Lx, 25.70.Pq

## I. INTRODUCTION

The isospin effects in intermediate energy heavy-ion collisions has been of unique interest from the last decade. The main motive of this detailed analysis is to get the rich information about symmetry energy and isospin-dependent nucleon-nucleon (NN) cross sections or in other terms determination of nuclear equation of state (NEOS) of asymmetric nuclear matter by studying the phenomenas of multifragmentation and collective flow [1–17]. In addition, the symmetry energy and isospin dependent cross sections play an important role in understanding many astrophysical and nuclear processes linked with neutron star, cooling processes at critical density as well as liquid gas phase transition[2, 18]. A couple of sophisticated experiments has been performed to look for the isospin effects, especially, in term of symmetry energy and many more are in progress in near future[4, 6, 8, 10, 14, 17]. The competitive progress is also done on the theoretical front[1–3, 5, 9, 11–13, 15, 16, 19, 20].

On the theoretical front, the dynamical models such as Quantum Molecular Dynamical (QMD)[21–23], Boltzmann Uehling Uhlenbeck (BUU) models [2] are used for the study of heavy-ion collisions at intermediate energies. No dynamical model simulates the fragments. Only the phase space of nucleons is obtained from the dynamical models and fragments are supposed to be constructed by using the secondary algorithms. In the efforts to reproduce the experimental data, many secondary algorithms has been developed time to time.

The most commonly and widely used algorithm depends on the spatial and momentum coordinates of the nucleons, is known as minimum spanning tree (MST) algorithm [7, 13, 22]. According to this method, two nucleons will undergo the cluster formation if the relative distance ($|R_i - R_j|$) and relative momentum ($|P_i - P_j|$) between the nucleons is less than 3.5-4 fm and 250-268 MeV/c, respectively. These parameters can be obtained by fitting the experimental data for some of the global observables such as multiplicity of intermediate mass fragments ($N_{IMFs}$)[22, 24]. Recently, MST method has been further extended to Isospin MST, in which the cut on the momentum space is kept same, but, the cut on the spatial coordinates is constraint on the basis of type of particles. The distance between the different kind of particles is taken as follow: $|R_i^p - R_j^p| \approx 3fm$, $|R_i^n - R_j^p| = |R_i^n - R_j^n| \approx 6fm$[25], where $p$, $n$ stands for protons and neutrons.

The MST method has been quite successful in explaining certain fragmentation observables such as charge distribution of emitted fragments[22, 26], single and double yield ratio of neutrons to protons[6, 7], while fails to describe some important detail in the production of free nucleons, light and heavy charged particles [22, 26–28]. The failure results are summarized as follow: (1) Yield of $Z = 1$ is overestimated, while $Z = 2$ is underestimated. (2) In Iso-Scaling phenomena, enhanced production of neutron-rich isotopes[29]? (3) neutron-rich light charged particles at mid-rapidity[30]? (4) Behaviour of $Z_{bound}$

*Author to whom all correspondence should be addressed: Sanjeev1283@gmail.com

†Electronic address: ygma@sinap.ac.cn

dependence of IMFs at high incident energy of 600 to 1000 MeV/nucleon[26, 28]? The studies in the literature shows that these results can not only reproduced by changing the mean field or NN cross sections in the transport model, keeping secondary algorithm same.

Since the MST method only depends on the constraints from position and momentum, so it seems to be worry about the stability of fragments due to the formation of artificial weakly bound fragments. To avoid from this problem, more complicated methods like Stimulated Annealing Clusterization Algorithm (SACA)[23], Early Cluster Recognization Algorithm (ECRA)[31] were also developed. These method were found quite successful , but, most complicated. Moreover, due to the choice of parameters such as cooling parameters, iterations procedure, and choice of minimal can follow the totally different configuration of fragments. Due to the limitation of sharp minimal, in the mildly excited or asymmetric systems, the scope of these two methods was found to restrict at some point. The best method for avoiding from the artificial formation of fragments is found to constraint the fragments by using an average binding energy cut of -4 MeV/nucleon[26]. One can further improve the method by using the realistic binding energy cut rather than -4 MeV/nucleon[26]. This method was found to be as simple as MST and found to reproduce the experimental data just like the complicated methods SACA, ECRA etc.

The isospin physics, which is new and exciting field in the present era, has been widely explored by using the simple MST method till 2013 [3, 7, 8, 13, 21]. Meanwhile, in 2012, the attempts were done by incorporating modifications in MST in term of spatial distance between the nucleons on the basis of type of particles[25]. The MSTB and other sophisticated methods in the literature were only coupled with the isospin-independent dynamical models. In these studies, MSTB, ECRA and SACA were also found to be lack of energy contribution from momentum dependent and symmetry potentials. With the availability of isospin dependent version of QMD model, it is the need of the present time to explore the isospin physics with other secondary algorithms except simple MST and Iso-MST.

In this work, first time, we have modified the MST method to MSTB including the energy contribution from momentum dependent and symmetry potentials in addition to Skyrme, Coulomb and Yukawa interactions. The effect of MSTB is studied by considering the neutron-rich systems $^{112}Sn +^{112} Sn$ and $^{124}Sn +^{124} Sn$ for the yield and single ratio of isospin sensitive particles such as n, p, $^3H$ and $^3He$.

The article is organized as follow: The short description of IQMD model coupled with secondary algorithm MSTB is discussed in Sec. II. The results and discussion are presented in Sec. III, followed by the conclusions in Sec. IV.

## II. THE FORMALISM

### A. Isospin Quantum Molecular Dynamics Model (IQMD)

In the present work, IQMD model is used for generating the phase space of nucleons [7, 13, 21]. The model is modified by the authors for the density dependence of the symmetry energy, having form:

$$E_{Sym}(\rho) \;=\; E_{Sym}^{Kin} \;+\; E_{Sym}^{Pot}$$

$$E_{Sym}(\rho) \;=\; \frac{C_{s,k}}{2}\left(\frac{\rho}{\rho_0}\right)^{2/3} \;+\; \frac{C_{s,p}}{2}\left(\frac{\rho}{\rho_0}\right)^{\gamma_i},$$

$E_{Sym}^{Kin}$ and $E_{Sym}^{Pot}$ are the symmetry kinetic energy and symmetry potential energy. The values of parameters $C_{s,k}$ and $C_{s,p}$ are 25 and 35.2 MeV, respectively. When we set $\gamma_i = 0.5$ and 1.5, respectively, it corresponds to the soft and stiff symmetry energy [7].

The total interaction potential is composed of Coulomb ($V_{\rm Coul}$), Yukawa ($V_{\rm Yukawa}$), local ($V_{\rm loc}$) and momentum dependent interactions ($V_{\rm MDI}$). The expressions for $V_{\rm Coul}$ and $V_{\rm Yukawa}$ have been derived by us and others [21]. The local interaction potential $V_{\rm loc}$ is originated from the Skyrme energy density function. On the basis of this, the local potential energy density is expanded as:

$$U_{\rm loc} \;=\; \frac{\alpha}{2}\frac{\rho^2}{\rho_0} \;+\; \frac{\beta}{\gamma+1}\frac{\rho^{\gamma+1}}{\rho_0^{\gamma}} + E_{\rm Sym}^{\rm pot}(\rho)\rho\delta^2, \qquad (1)$$

where $\alpha$, $\beta$, and $\gamma$ are the parametrized values to specify the particular NEOS. The detailed table of the values is presented in the Ref. [21, 22].

The momentum dependent potential has been implemented from Ref.[22] and is expressed as following: $V_{\rm MDI} = C_{\rm mom}\ln^2[\epsilon(\Delta p)^2+1]\frac{\rho}{\rho_0}\delta(r'-r)$. Here $C_{\rm mom} =$ 1.57 MeV and $\epsilon = 5\times10^{-4}\frac{c^2}{MeV^2}$. The momentum is given in units of MeV/c.

Finally, combining all the potentials, we got an isospin, density and momentum dependent single particle potential in nuclear matter, which is written as follow:

$$\begin{aligned} V_\tau(\rho,\delta,p) \quad &= \alpha\left(\frac{\rho}{\rho_0}\right) + \beta\left(\frac{\rho}{\rho_0}\right)^{\gamma} + E_{\rm Sym}^{\rm pot}(\rho)\delta^2 \\ &+\frac{\partial E_{\rm Sym}^{\rm pot}(\rho)}{\partial\rho}\rho\delta^2 + E_{\rm Sym}^{\rm pot}(\rho)\rho\frac{\partial\delta^2}{\partial\rho_{\tau,\tau'}} \\ &+C_{\rm mom}\ln^2[\epsilon(\Delta p)^2+1]\frac{\rho}{\rho_0}. \end{aligned} \qquad (2)$$

Here $\tau\neq\tau'$, $\frac{\partial\delta^2}{\partial\rho_n} = \frac{4\delta\rho_p}{\rho^2}$, and $\frac{\partial\delta^2}{\partial\rho_p} = \frac{-4\delta\rho_n}{\rho^2}$.

In the present simulations, the parameters $\alpha$, $\beta$, and $\gamma$ are -390, 320 MeV and 1.14, respectively. Moreover, the isospin and energy dependent NN cross section in the collision term and the quantum feature in term of Pauli blocking is implemented.

The Improved QMD (ImQMD) model, which is used in Refs. [6, 25] and our IQMD model are based on the similar basic theory of QMD model developed by Aichelin in 1991 [22]. During the modification of QMD to ImQMD and IQMD some differences are observed in term of Yukawa Potential form, system mass dependent Gaussian width, symmetry energy dependent/independent momentum dependent interactions and shell correction factor. Due to the difference in the two models on the basis of above mentioned factors, the partial difference can be seen in the results [7].

### B. Minimum Spanning tree method with binding energy check(MSTB)

This method is a modified version of the normal MST and old MSTB method. The difference between old MSTB and this MSTB is the additional contribution of energy from momentum dependent interactions and symmetry potentials in the calculation of total binding energy. The procedure is as follow: The phase space obtained from IQMD is analyzed with simple MST method and pre-clusters are short out. We are not aware about the stability of pre-clusters formed at this stage. So, the pre-clusters formed from simple MST are now subjected to the binding energy condition as follow:

$$\zeta = \frac{1}{N_f}\sum_{\alpha=1}^{N_f}\left[\sqrt{\left(\mathbf{p}_\alpha - \mathbf{P}_{N_f}\right)^2 + m_\alpha^2} - m_\alpha + \frac{1}{2}\sum_{\beta\neq\alpha}^{N_f} V_{\alpha\beta}\right] \quad (3)$$

$$\zeta < -E_{bind} \quad (4)$$

Here, we take $E_{bind} = 4.0$ MeV/nucleon if $N_f \geq 3$ and $E_{bind} = 0$ otherwise. In this equation, $N_f$ is the number of nucleons in a fragment, $P_{N_f}$ is the average momentum of the nucleons bound in the fragment. The requirement of a minimum binding energy excludes loosely bound fragments which will decay later. The realistic value of $E_{bind}$ changes slightly the fragment multiplicity at intermediate times, but has no influence on the quantitative behavior and on the asymptotic results. However, if by using the realistic binding energy, one searches for the most bound configuration, the results are found to affect. At the present time, we had just focused on the bound configurations and hence the average cut of binding energy -4 MeV/nucleon is justified.

If any pre-cluster fails to meet the binding energy condition in Eqs. 3 and 4, this pre-cluster is treated as unbound and all the nucleons of such type of pre-cluster are treated as free nucleons. Naturally, the artificially or locally bounded fragments will be automatically discarded in the new MSTB method.

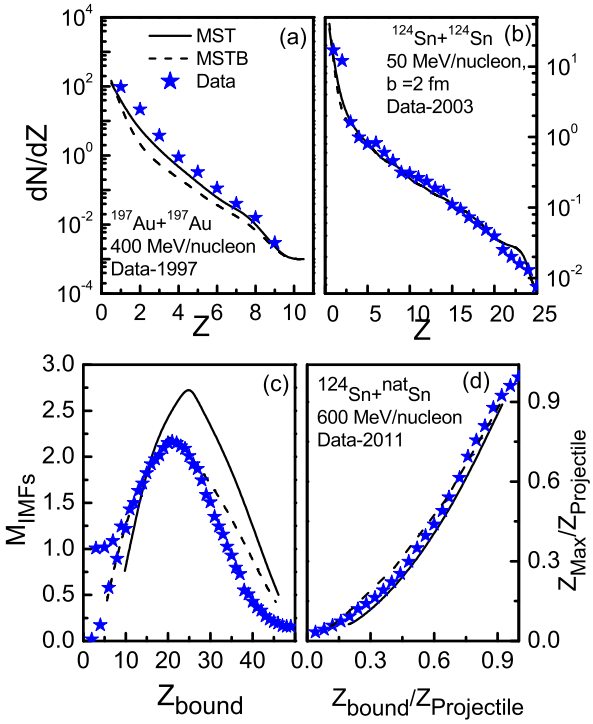


FIG. 1: (Color online)(i)The upper panels: Comparison of charge distribution of experimental data of $^{197}Au + ^{197}Au$ and $^{129}Xe + ^{nat}Sn$ with the results obtained using MST and MSTB algorithms. Here the theoretical calculations are of $^{124}Sn + ^{124}Sn$ for right panel. (ii)In the bottom left (right) panels, the comparison of the results of $Z_{bound}(Z_{bound}/Z_{projectile})$ dependence of $M_{IMFs}(Z_{Max}/Z_{Projectile})$ with the experimental data of GSI for the projectile fragmentation of $^{124}Sn$.

## III. RESULTS AND DISCUSSION

For the present study, thousands of event of $^{112}Sn + ^{112}Sn$, $^{124}Sn + ^{124}Sn$ at central impact parameter between the incident energy 50 and 600 MeV/nucleon are simulated using the IQMD model coupled with MST and MSTB algorithm. For the preliminary comparison of theoretical calculations with experimental data the reactions of $^{197}Au + ^{197}Au$ (at 400 MeV/nucleon for central collisions) [32] and $^{124}Sn + ^{nat}Sn$ (at 600 MeV/nucleon throughout the collision geometry)[33] are also simulated. By checking the validity of MSTB through the comparison of our results with experimental data, the detailed analysis of rapidity and kinetic energy spectra of isospin sensitive particles such as neutrons (n), protons (p), triton($^3H$), helium ($^3He$)is presented.

In Fig.1, the comparison of experimental data of charge distribution and $Z_{bound}$ dependence of multiplicity of intermediate mass fragments ($M_{IMFs}$), $Z_{Max}$ with the calculations of MST and MSTB algorithm is displayed. The charge distribution is displayed for

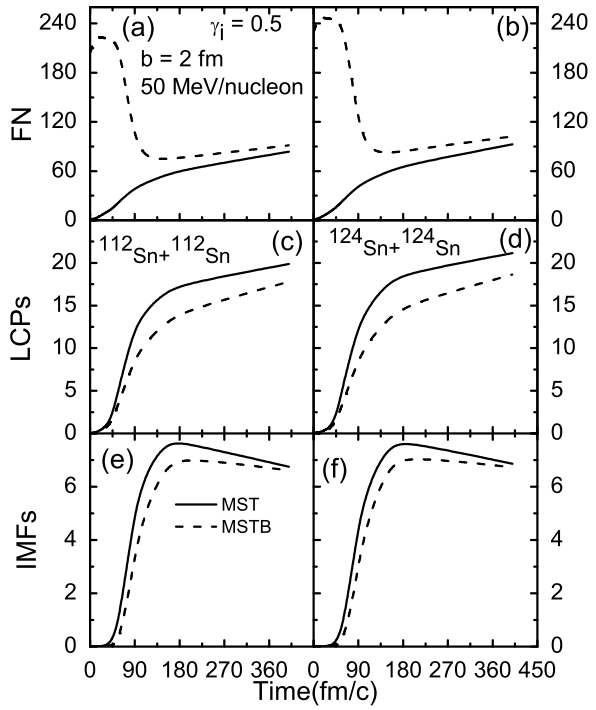


FIG. 2: The time evolution of different kind of fragments: free nucleons (upper), LCPs(middle), and IMFs(bottom) panels for central collisions at 50 MeV/nucleon with MST and MSTB algorithms. The left (right) panels are for neutron-poor (neutron-rich) $^{112}Sn + {}^{112}Sn$ ($^{124}Sn + {}^{124}Sn$) reaction systems. All the results are with soft symmetry energy.

$^{197}Au + {}^{197}Au$ at 400 MeV/nucleon [32] (left upper panel) and $^{124}Sn + {}^{124}Sn$ at 50 MeV/nucleon (right upper panel)[34]. The charge distribution at 50 MeV/nucleon is well reproduced by MST as well as MSTB algorithms, while at 400 MeV/nucleon, the data is little underestimated by MSTB. It is not surprising since it is well known that MSTB method can not create additional fragments, rather, it refines the fragments and hence results are logically true. Furthermore, when the recent available experimental data of $Z_{bound}$ dependence of $M_{IMFs}$ and $Z_{max}$ is compared with MST and MSTB calculations, the importance of MSTB is clearly visible. In our recent communication[13], hard equation of state with MST reproduces the data, can be discarded on the basis of present results. The present results clearly indicate that the soft equation of state with MSTB method can reproduce the experimental data. The results obtained are as reliable as obtained by SACA in the previous studies[35]. This is also true for the $Z_{bound}$ dependence of $Z_{Max}$. From the comparison, one can say that except the adjustment of mean field and collision part in term of soft and hard equation of state, it is worth important to develop some secondary algorithms for the proper understanding of nuclear physics phenomenas and nuclear equation of state.

In Fig.2, the time evolution of free particles, LCPs and IMFs for neutron-poor and neutron-rich reaction system at 50 MeV/nucleon with MST and MSTB algorithms is displayed. In the high density phase, the MSTB algorithm does not find any fragment with reasonable binding energy and hence most of the particles are free, while there were a lot of artificial fragments with MST. After the high density phase is over, it starts recognizing the fragments, which are real, bound and stable. In all the cases, MSTB helps to identify the fragments quite early. From the figure, it is clear that MSTB enhances the production of free particles and reduces the production of LCPs and IMFs. Moreover, with increase in the size of the fragment, MST takes less time to match with the MSTB results and also the difference between MST and MSTB results goes on decreasing throughout the time evolution.

During the comparison of results between neutron-poor and neutron-rich reaction system, it is found that enhanced production of fragments takes place for the more neutron-rich system. The enhanced production is sensitive for free nucleons and LCPs compared to IMFs. It is also shown by us recently that free nucleons and LCPs are more sensitive towards the symmetry energy compared to IMFs[13]. In this regard, the sensitivity of free nucleons and LCPs with MSTB towards the neutron-rich system can also play an important role in the prediction of symmetry energy, which is a topic of separate discussion. For the further study, the isospin sensitive free nucleons and LCPs, namely, n, p, $^3H$ and $^3He$ are used.

In the literature, isospin effects, especially, symmetry energy has been predicted by using the rapidity and kinetic energy spectra of yield, ratio or flow of different kind of isobaric or isotopic particles[2, 7, 11]. Following the same, in Figs. 3 (4), we display the rapidity distribution (kinetic energy spectra) of isospin sensitive particles n, p, $^3H$ and $^3He$ with MST and MSTB algorithms for neutron-poor as well as neutron-rich reaction systems. In addition, the differential distribution is also plotted in the extreme right panel of both the figures. In Fig. 3, with the increase in isospin of the system, the results with MSTB (MST) affects the yield of neutron-rich (proton rich) particles i.e. neutrons and $^3H$ (protons and $^3He$) over all the rapidity region, especially at mid-rapidity. This is indicating the weak (strong) contribution of Coulomb effects (symmetry energy) with MSTB compared to MST. These finding are strengthening MSTB a good method towards the better understanding of the symmetry energy.

The clear isospin effects can be seen from the differential rapidity distribution of (n-p) and ($^3H - {}^3He$). For neutron-rich system, quite strong sensitivity can be seen of the differential distribution compared to individual yield distribution with MSTB. This is true for the (n-p) as well as ($^3H - {}^3He$) differential rapidity distribution.

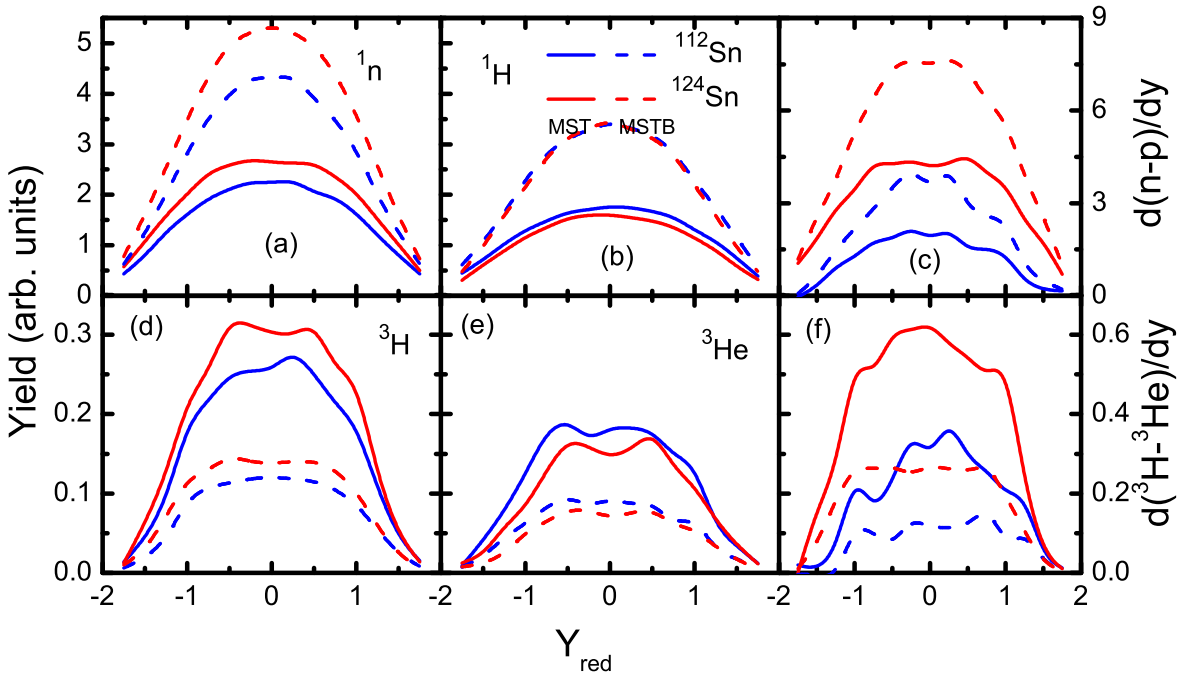


FIG. 3: (Color online) The rapidity distribution of neutrons, protons, $^3H$ and $^3He$ particles for neutron-poor and neutron-rich reaction systems with MST and MSTB algorithms. The results for the differential rapidity distribution of (n-p) and ($^3H$ − $^3He$) are also presented in the right top and bottom panels, respectively.

Lets move towards the kinetic energy distribution (Fig.4). The sensitivity towards method of clusterization and isospin physics, collectively, is observed at lower end of kinetic energy spectra of neutrons and diffrential (n-p), however, at higher kinetic energies, spectra is only sensitive towards the isospin physics and not toward method of clusterization. Due to the low yield of $^3H$ and $^3He$ particles at 50 MeV/nucleon, it is hard to identify the isospin effects. It is concluded that free neutrons individual, n-p ($^3H - ^3He$ ) differential spectra at low (high) kinetic energy as well as at mid-rapidity affects the results significantly with MSTB over MST method.

In order to elaborate the kinetic energy spectra further, the kinetic energy dependence of single ratios is shown in Figs. 5 at 50 MeV/nucleon. In Fig. 5, more MSTB effects has been observed for neutron-rich system throughout the kinetic energy for single neutrons to protons ratio. As discussed earlier, the sensitivity of MSTB over MST is decreasing towards the higher kinetic energy, is also true here. No any systematic is observed with the present data for $^3H/^3He$. The statistics need to be improved for this in near future. The higher single ratio with simple MST algorithm is due to the decreased production of protons and not much neutrons for the neutron-rich system. The real strength of symmetry energy is to enhance the production of neutrons due to repulsive nature. The binding energy algorithm enhances (decreases) the production of neutrons (protons) to great (weak) extent towards the neutron-rich system. The weak sensitivity of MSTB towards the protons production is justified as the reaction systems $^{112}Sn$ and $^{124}Sn$ has same number of protons and different neutrons. It strengthen to include the binding energy effects for the proper understanding of isospin effects due to symmetry energy. One must take caution when they consider the enhanced single neutrons to protons ratio with simple MST as a signature of symmetry energy.

For better understanding, one must check the sensitivity of yield contribution of different particles using the linear or power law fit method. In Fig.6, the isospin asymmetry dependence of yield of different particles and corresponding ratios is fitted with the power law of the form $Y = AX^{\tau}$. The numerical values in the figure shows the value of the power law parameter $\tau$. The production of neutron-rich (proton-rich) particles n, $^3H$ (p,$^3He$) is increasing (decreasing) with isospin asymmetry of the system for MST as well as MSTB algorithm. In comparison of neutron-rich particles, n ($^3H$) production is more sensitive with MSTB (MST) algorithm, however, in comparison of proton-rich particles p($^3He$) are more

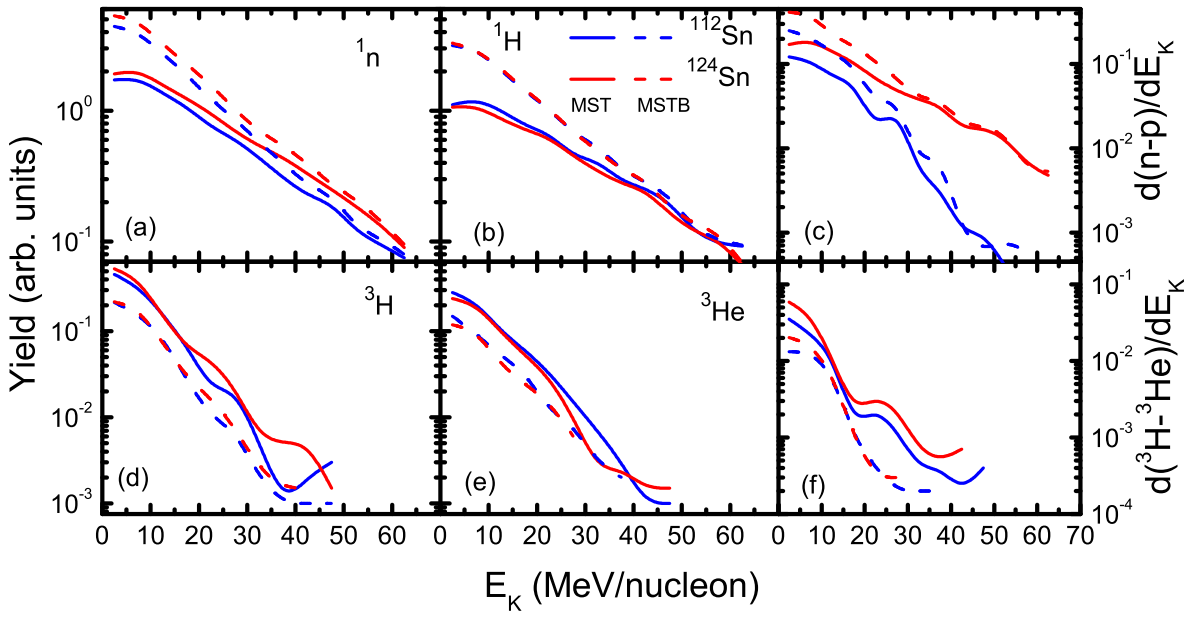


FIG. 4: (Color online) Same as in Fig.3, but for the kinetic energy dependence instead of rapidity distribution dependence.

sensitive with MST (MSTB) algorithm. It is indicating $^3H$ and $^3He$ produced with simple MST are greatly unstable. Especially, it is true for $^3He$ particles, which is already verified from physics point of view. Furthermore, the sensitivity of $n/p$ ($^3H/^3He$) ratio is high with MST method. Interestingly, the sensitivity parameter difference of MST over MSTB is quite strong for $n/p$ compared to $^3H/^3He$. This difference motivated us to study the same sensitivity towards the high incident energy.

Just like the Fig.6, the isospin asymmetry dependences of $n/p$ and $^3H/^3He$ is fitted towards the high incident energies of 100, 200, 400 and 600 MeV/nucleon with the power law. The incident energy dependence of power law parameter $\tau$ is shown in Fig.7. The sensitivity of $n/p$ ($^3H/^3He$) with the incident energy is decreasing (zig-zag motion). For $n/p$, it is due to the importance of other degree of freedoms such as meson production and nucleon resonances towards the high incident energy. Upto 1 GeV/nucleon, the Ultra-relativistic QMD (UrQMD) [38] as well as IQMD [21] can explain the experimental GSI data with a good degree of accuracy. For the better reproduction of experimental data with IQMD model on and above 600 MeV/nucleon till 1GeV/nucleon, the different kind of clusterization methods also plays quite important role [26, 35]. In addition, UrQMD, in which meson production and nucleon resonances are well treated, has been able to explain the experimental data above 1 GeV/nucleon also, where IQMD model fails badly. For $^3H/^3He$, the zig zag behavior with incident energy is due to the platue formation for LCPs production around 400 MeV/nucleon[36]. The sensitivity of $n/p$ ($^3H/^3He$) with MSTB is decreasing (increasing) towards the high incident energy, which is quite interesting observation. The study is clearly indicating that the contribution of different type of particles towards the isospin physics at higher incident energies with different clusterization methods is found to vary drastically. [37].

## IV. CONCLUSION

In conclusion, we have introduced, first time, a clusterization method with binding energy cut coupled with IQMD in order to understand the isospin physics. However, the binding energy clusterization methods like MSTB, SACA were also used earlier for the study of many phenomena's in heavy-ion collisions at intermediate energies [23, 26, 31, 35], but not for the study of isospin physics. The importance of present MSTB method is as follow: 1. The contribution of energy from momentum dependent interactions and symmetry potential is included during the calculation of total binding energy of fragments, which is affecting the actual yield of fragments compared to earlier MSTB method. 2. When the method is applied to isospin sensitive fragments, the drastic variation in the results can be seen, which was never checked with this method earlier.

The detailed results are presented below. With this

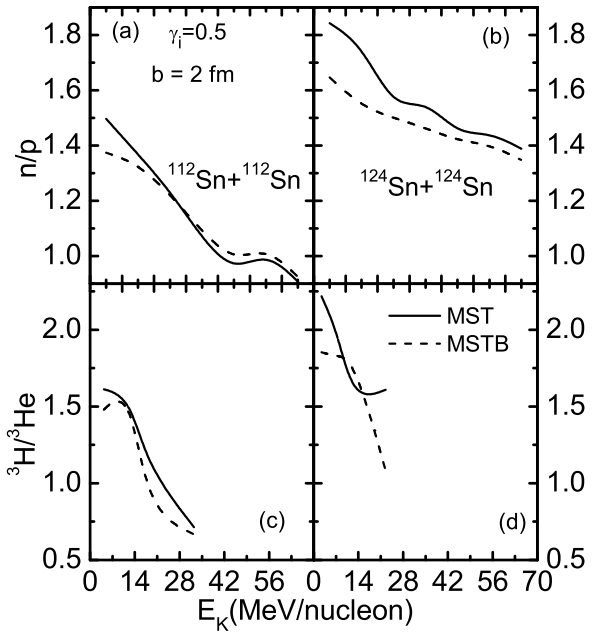


FIG. 5: The kinetic energy dependence of single n/p ($^3H/^3He$) in top (bottom) panels for neutron-poor and neutron-rich reaction systems with MST and MSTB algorithms.

method, we found enhanced production of free nucleons, while decreased production of light charged particles. The free nucleons enhancement is mostly found to contributed from the symmetry energy sensitive particle i.e. neutrons. The absolute and differential yield of isospin sensitive particles n,p, $^3H$ and $^3He$ is found to be greatly affected by MSTB in mid rapidity and low kinetic energy region. The magnitude of kinetic energy dependence of single neutrons to protons ratio is found to be decrease with MSTB and is mostly affected for the neutron-rich system. The yield sensitivity with MSTB method towards high incident energy is found to decrease (increase) for $n/p$ ($^3H/^3He$). The sensitivity at high incident energy need to be tested in near future. In conclusion, the binding energy cut is of utmost importance in heavy-ion collisions at intermediate energies in order to understand the isospin physics and stability of fragments.

## ACKNOWLEDGMENTS

This work is supported in part by the Chinese Academy of Sciences Support Program for young international scientists under the Grant No. 2010Y2JB02,

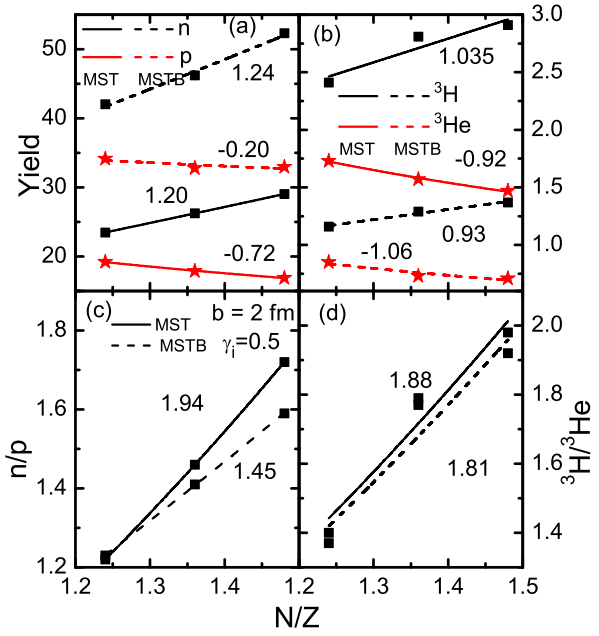


FIG. 6: (Color online) Isospin asymmetry dependence of yield of neutrons, protons ($^3H$ and $^3He$) with MST and MSTB algorithms in top left (right) panels. The corresponding n/p ($^3H/^3He$) dependence is shown in bottom left (right) panels. All the lines are fitted with power law of the form $Y = AX^\tau$.

the National Science Foundation of China under contract No.s 11035009, 10979074, and the Knowledge Innovation Project of the Chinese Academy of Sciences under Grant No. KJCX2-EW-N01.

[1] S. Gautam, R. Kumari, and R. K. Puri, Phys. Rev. C **86**, 034607 (2012).
[2] B. A. Li, L. W. Chen, and C. M. Ko, Phys. Rep. **464**, 113 (2008) .
[3] A. Jain, S. Kumar, and R. K. Puri, Phys. Rev. C **85**, 064608 (2012).
[4] J. B. Natowitz *et al.,* Phys. Rev. Lett. **104**, 202501 (2010); L. Qin *et al.,* Phys. Rev. Lett. **108**, 172701 (2012) .
[5] S. Gautam, A. D. Sood, R. K. Puri, and J. Aichelin, Phys. Rev. C **83**, 034606 (2011).
[6] M. B. Tsang *et al.,* Phys. Rev. Lett. **102**, 122701 (2009);

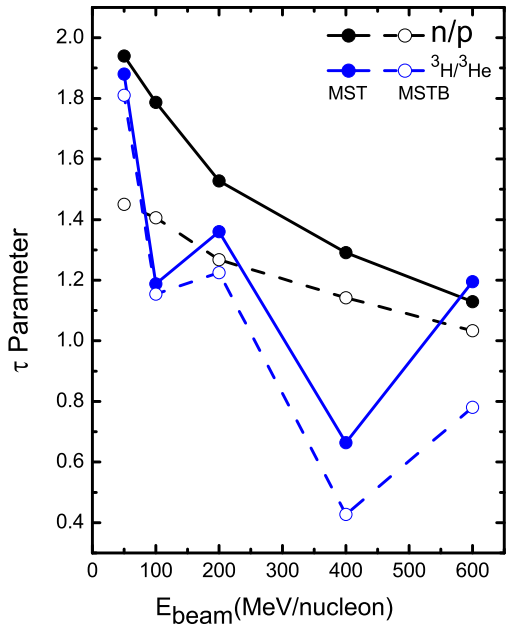


FIG. 7: (Color online) Incident energy dependences of the power law fitted parameter $\tau$(from isospin asymmetry dependence of n/p and ($^3H/^3He$) at different incident energies) with MST and MSTB algorithms.


D. D. S. Coupland *et al.,* Phys. Rev. C **84**, 054603 (2011).

[7] S. Kumar, Y. G. Ma, G. Q. Zhang, and C. L. Zhou, Phys. Rev. C **84**, 044620 (2011); *ibid.* Phys. Rev. C **85**, 024620 (2012).

[8] Z. Y. Sun *et al.,* Phys Rev. C **82**, 051603 (R) (2010).

[9] Z. G. Xiao, B. A. Li, L. W. Chen, G. C. Yong, and M Zhang, Phys. Rev. Lett. **102**, 062502 (2009) .

[10] P. Russotto *et al.,* Phys. Lett. B **697**, 471 (2011).

[11] Z. Q. Feng, Phys. Lett. B **707**, 83 (2012).

[12] W. J. Xie, J. Su, Z. Zhu, and F. S. Zhang, Phys. Lett. B **718**, 1510 (2013).

[13] S. Kumar and Y. G. Ma, Nucl. Phys. A **898**, 59 (2013).

[14] M. B. Tsang *et al.,* Phys. Rev. Lett. **92**, 062701 (2004); M A Famiano *et al.,* Phys. Rev. Lett. **97**, 052701 (2006).

[15] B. A. Li, Phys. Rev. Lett. **88**, 192701 (2002).

[16] B. A. Li, L. W. Chen, H. R. Ma, J Xu, and G C Yong, Phys. Rev. C **76**, 051601 (R) (2007).

[17] F. Amorini *et al.,* Phys. Rev. Lett. **102**, 112701 (2009).

[18] J M Lattimer and M Prakash, Science **304**, 536 (2004); D. T. Loan *et al.,* Phys. Rev C **83**, 065809 (2011).

[19] S. S. Bao and H. Shen, Phys. Rev. C **89**, 045807 (2014).

[20] Y. Wang *et al.,* Phys. Rev. C **89**, 044603 (2014).

[21] C Hartnack *et al.,* Eur. Phys. J. A **1**, 151 (1998).

[22] J. Aichelin, Phys. Rep. **202**, 233 (1991); E. Lehmann *et al.,* Prog. Part. Nucl. Phys. **30** , 219 (1993).

[23] R. K. Puri and J. Aichelin, J. Comput. Phys. **162** , 245 (2000).

[24] J. Singh and R. K. Puri, Phys. Rev. C **62**, 054602 (2000).

[25] Y. Zhang *et al.,* Phys. Rev. C **85**, 051602 (2012).

[26] S. Goyal and R. K. Puri, Phys. Rev. C **83**, 047601 (2011).

[27] R. Nebauer *et al.,* Nucl. Phys. A **658**, 67 (1999).

[28] S. Kumar and S. Kumar, Pramana J. of Phys. **74**, 731 (2010).

[29] T. X. Liu *el al.,* Phys. Rev. C **69**, 014603 (2004).

[30] Z. Kohley *et al.,* Phys. Rev. C **83**, 044601 (2011).

[31] C. O. Dorso and J. Randrup, Phys. Lett. B **301** 328 (1993).

[32] W. Reisdorf *et al.,* Nucl. Phys. A **612**, 493 (1997).

[33] R. Ogul *et al.,* Phys. Rev. C **83**, 024608 (2011).

[34] S. Hudan *et al.,* Phys. Rev. C **67**, 064613 (2003).

[35] Y. K. Vermani and R. K. Puri, Europhys. Lett. **85**, 62001 (2009).

[36] S. Kumar, S. Kumar, and R. K. Puri, Phys. Rev. C **81**, 014601 (2010).

[37] S. Kumar and R. K. Puri, Phys. Rev. C **58**, 2858 (1998).

[38] Q. F. Li, Z. Li, E. Zhao and R. K. Gupta, Phys. Rev. C **71**, 054907 (2005); H. Peterson, Q. Li, X. Zhao and M. Bleicher, Phys. Rev. C **74**, 064908 (2006); Y. Yuan, Q. Li, Z. Li and F. H. Liu, Phys. Rev. C **81**, 069901 (2010); Q. Li *et al.*, Phys. Rev. C 83, 044617 (2011); G. Graf, M. Bleicher and Q. Li, Phys. Rev. C **85**, 044901 (2012).